

METHODOLOGY FOR ASSESSING AND CONTROLLING THE RISK GRADE OF STRUCTURAL COLUMNS THREATENED BY BLAST INCIDENT

Peng SUN^{1,2}, Xiaomeng HOU^{1,2,3}✉

¹Key Lab of Structures Dynamic Behavior and Control of the Ministry of Education, Harbin Institute of Technology, 150090 Harbin, China

²Key Lab of the Smart Prevention and Mitigation of Civil Engineering Disasters of the Ministry of Industry and Information Technology, Harbin Institute of Technology, 150090 Harbin, China

³Key Lab of Building structural Retrofitting and Underground Space Engineering of the Ministry of Education, Shandong Jianzhu University, 250101 Jinan, China

Article History:

- received 4 November 2023
- accepted 16 March 2025

Abstract. Columns are important structural components and are threatened by local conflicts and explosion accidents. This paper presents a fuzzy-based risk assessment framework to evaluate the potential blast disasters associated with structural columns. The framework establishes an indicator system and incorporates risk functions and a fuzzy transformation system for blast risk assessment. The priority weights of critical attributes are determined using a fuzzy analytic hierarchy process (FAHP) approach, and the risk factor (RF) is calculated via the aggregation of foundational fuzzy evaluations. The feasibility and applicability of the framework are demonstrated through the risk level assessment of five example columns. The framework's rationality is further validated by comparing the onrisk grades of identical cases, as assessed by the proposed framework and alternative methods. The study results indicated that the framework can effectively discern the risk range of desired grade rankings and ascertain the risk grade. By integrating the obtained attribute ranking and hierarchical structure, the framework facilitates the identification of potent strategies for controlling blast risk. The resulting risk-grade findings serve as a foundation for the identification of priority protection and anti-explosion design of structural columns.

Keywords: blast disaster, multi-criteria risk assessment, fuzzy theory, structural column.

✉Corresponding author. E-mail: houxiaomeng@gmail.com

1. Introduction

In recent years, the increases in terrorist attacks and local wars represented by the Israeli-Palestinian and the Russia-Ukraine conflict worldwide (Qi et al., 2017; Ouyang, 2014; Yan et al., 2022), in addition to incidents of explosive material accidents during production, storage, and transportation (Sun et al., 2022; Li et al., 2022), have elevated the risk to engineering structures from potential blast incidents. Structural columns, key load-bearing components of civil engineering, are not generally equipped with anti-explosion facilities and are easily accessible (Shi & Stewart, 2015; Zhou et al., 2022; Hou et al., 2018). Thus, in the event of an explosion, these columns can sustain significant damage, potentially leading to a cascading collapse of the structure (Gündel et al., 2012; Stawczyk, 2003; Shi et al., 2010). Therefore, there is an increasing need to develop methods for evaluating and controlling the blast disasters to these columns.

The risk level of engineering structures being subjected to an explosion accident varies, it is consequential to identify high-risk columns as priority targets for retrofitting (Clough & Clublely, 2019; Tetougueni et al., 2020). Moreover, some columns maintain their load-bearing capacity even when the structure sustains damage from an explosion (Wang & Zhang, 2022). Therefore, conducting an anti-explosion design for all columns is economically impractical. Risk assessment offers a risk grade by combining the disaster occurrence probability, disaster consequences, and the components' resistance performance (Koohathongsumrit & Meethom, 2024; Cho et al., 2023; Li et al., 2019).

To the best of our knowledge, this is the first study to quantitatively evaluate the risk level of columns subjected to blast disasters. Its novelty lies in establishing the indicator system of blast risk assessment and proposing

a framework for reasonably determining and controlling the blast risk grade. The blast risk grade can guide the definition of the fortification target and the strengthening strategy. The findings of this paper provide a basis for the monitoring of blast risk and performance-based blast-resistant design of structural columns.

2. Literature review

The conceptual definitions, risk functions, and evaluation methods of risk assessment vary across different fields (Qie & Rong, 2017; Pérez-Fernández et al., 2015; Davidson et al., 2006). The assessments of various disasters within the civil engineering field have been addressed in numerous studies (Zhen et al., 2022; Faber & Stewart, 2003; Wang & Elhag, 2007). Zhen et al. (2022) designed an indicator-based risk assessment framework for rural buildings exposed to flash floods. The flood disaster and building vulnerability were identified as the risk parameters of this indicator system. The weight of each indicator was calculated by combining the hierarchical analytical process and the random forest algorithm. Subsequently, the flood risk of rural buildings was quantitatively evaluated through a weighted aggregation process. Attary et al. (2017) introduced a performance-based framework to evaluate the risk tsunamis pose to structures in coastal communities. The probability and consequences of tsunami risk were determined by hazard analysis, structural vulnerability analysis, and loss analysis. The probabilistic framework can account for the randomness of disaster occurrence, construction materials, and structural parameters in assessing disaster risk. Tang et al. (2024) improved the failure mode and effects analysis (FMEA) model by combining the Dempster-Shafer evidence theory with grey relational projection method for risk management. The assessments of experts on risk indicators were modeled by the probability assignment function. The priority order of failure modes was ranked based on the grey relational projection method. The improved FMEA model effectively improved the accuracy and reliability in risk analysis. Although extensive research has been conducted on earthquake, tsunami, and flood risk assessment for structures, studies on blast risk for columns remain limited (Attary et al., 2017; Tang et al., 2024; Abdollahzadeh & Faghihmaleki, 2017). Disaster risk assessment methods can be primarily divided into three categories. The main advantage of the probabilistic framework is its ability to articulate performance indices (Attary et al., 2017; Qin & Stewart, 2020). However, as hazard analysis and structural damage probability are based on statistical data, these frameworks are unsuitable for disasters with irregular occurrence frequencies. The second category evaluates risk levels based on the simulation of disaster scenarios (Qie & Rong, 2017; Valdano et al., 2015). These frameworks address the issue of insufficient historical data but necessitate a clear understanding of the formation mechanism of each disaster scenario. The third category assesses the risk of extreme events with complex disaster

scenarios by selecting appropriate indicators (Zhen et al., 2022; Ravankhah et al., 2021). These frameworks only require that the indicators at the same level be independent of each other. In terms of rationality and effectiveness, the indicator-based method is suitable for risk assessments of structural members threatened by unconventional emergencies.

Calculating attribute weights and quantifying identified indicators are key processes in the multi-attribute risk assessment method. Attribute weighting methods are primarily divided into subjective and objective categories, including the hierarchical analytical process (AHP) (Mutlu & Sari, 2022), the principal component analysis (Ezcurra, 2024), the probabilistic analysis (Stewart & Netherton, 2008), factor analysis (Takaki & Gotoh, 2020), correlation coefficient-based methods (Tang et al., 2023) and machine learning-based approaches (Chen, 2021). The priority weights derived from subjective methods depend on the judgment of decision-makers, while objective methods tend to overlook the effects of data characteristics among different indicators. The risk level of columns exposed to blast incidents is influenced by numerous attributes, some of which present a degree of fuzziness and uncertainty. The fuzzy theory has been employed to manage ambiguity in the quantification process of qualitative indicators (Chen, 2001; Wang & Elhag, 2006; Ji et al., 2015). Wang and Elhag (2006) developed a fuzzy TOPSIS framework based on alpha-level sets for bridge risk assessment. The fuzzy linguistic terms describing the risk parameters were determined based on expert systems. The fuzzy analytic hierarchy process (FAHP) was used to calculate the weights of the attributes. The risk level of bridges was ranked by comparing the alpha level sets of the fuzzy relative closeness. Wang et al. (2011) established the hierarchical structure for flood risk assessment using the Delphi method. The priority weights of the indicators were calculated by the FAHP method, and spatial multi-criteria analysis was adopted to aggregate the quantitative indicators. The risk range was distinguished using the standard deviation method, and the flood risk distribution of a community was obtained. The FAHP method can address the imprecision of evaluation elements and diminish the effect of subjectivity on weight calculation. A review of existing literature affirms the rationality of the FAHP approach in calculating the weight of critical indicators (Wang et al., 2011; Kong & Zhang, 2024). As for the fuzzy evaluation of indicators, the membership functions (MFs) of linguistic variables were not unified. Most research compared the relative risk level of the object under study yet did not provide the criteria for determining risk grades. Studies on automatically and objectively outputting fuzzy evaluations based on the fundamental information of structural columns remain scarce.

Based on the above literature, this paper presents a universally applicable method to quantitatively assess the blast risk for columns in different areas. The fuzzy evaluations are obtained by associating linguistic terms, sub-

attributes of attributes, and fuzzy membership functions. The priority weight of each indicator is calculated using the FAHP method. The proposed indicator-based framework is employed for the blast risk assessment of the columns by taking five engineering structures in different areas as examples. This framework can manage quantitative and qualitative indicators and provide useful strategies for disaster management.

3. Research methods and materials

This section illustrates the proposed framework for evaluating the blast risks of columns. The method consists of two primary phases: 1) indicator system of blast risk assessment and 2) multi-indicator risk assessment framework. The specific procedures of each phase are described in the following subsections.

3.1. Phase 1: Indicator system of blast risk assessment

The parameters commonly employed in risk assessment mainly investigate the probability of a specific risk transpiring and the potential ramifications of the risk (Faber & Stewart, 2003; Karimi & Hüllermeier, 2007). These parameters, however, neglect to account for the influence of structural resistance performance. Zhen et al. (2022) and Ravankhah et al. (2021) proposed a parameter labeled 'explosion vulnerability' to address the blast performance of

columns. Consequently, the risk function is expressed as the multiplication of three risk parameters: column explosion vulnerability (B_1), blast consequence (B_2), and blast likelihood (B_3). The indicators contributing to the risk level of columns can be discerned and categorized in accordance with these risk parameters. The attributes under each risk parameter should remain independent. Figure 1 illustrates the hierarchical structure of the multi-attribute risk assessment. The attributes and sub-attributes are explained in detail below.

(1) Explosive vulnerability

Explosion vulnerability primarily pertains to the blast performance of columns. The attributes under this risk parameter can be inferred from research on column blast response and anti-explosion specifications.

■ Section area (C_1)

The column's dimensions and basic design parameters profoundly influence the column's blast performance (Sun et al., 2022). The section area is chosen to evaluate the column's blast performance due to the variety of cross-sectional shapes. The potential section area of the column can be $< 0.25 \text{ m}^2$, $0.25\text{--}1.00 \text{ m}^2$, $1.00\text{--}2.25 \text{ m}^2$, between $2.25\text{--}4.00 \text{ m}^2$, or $> 4.00 \text{ m}^2$ (Sun et al., 2021).

■ Slenderness ratio (C_2)

The failure mode of columns under blast loading is impacted by the slenderness ratio (Al-Thairy, 2016). Columns with a high slenderness ratio are susceptible to flex-

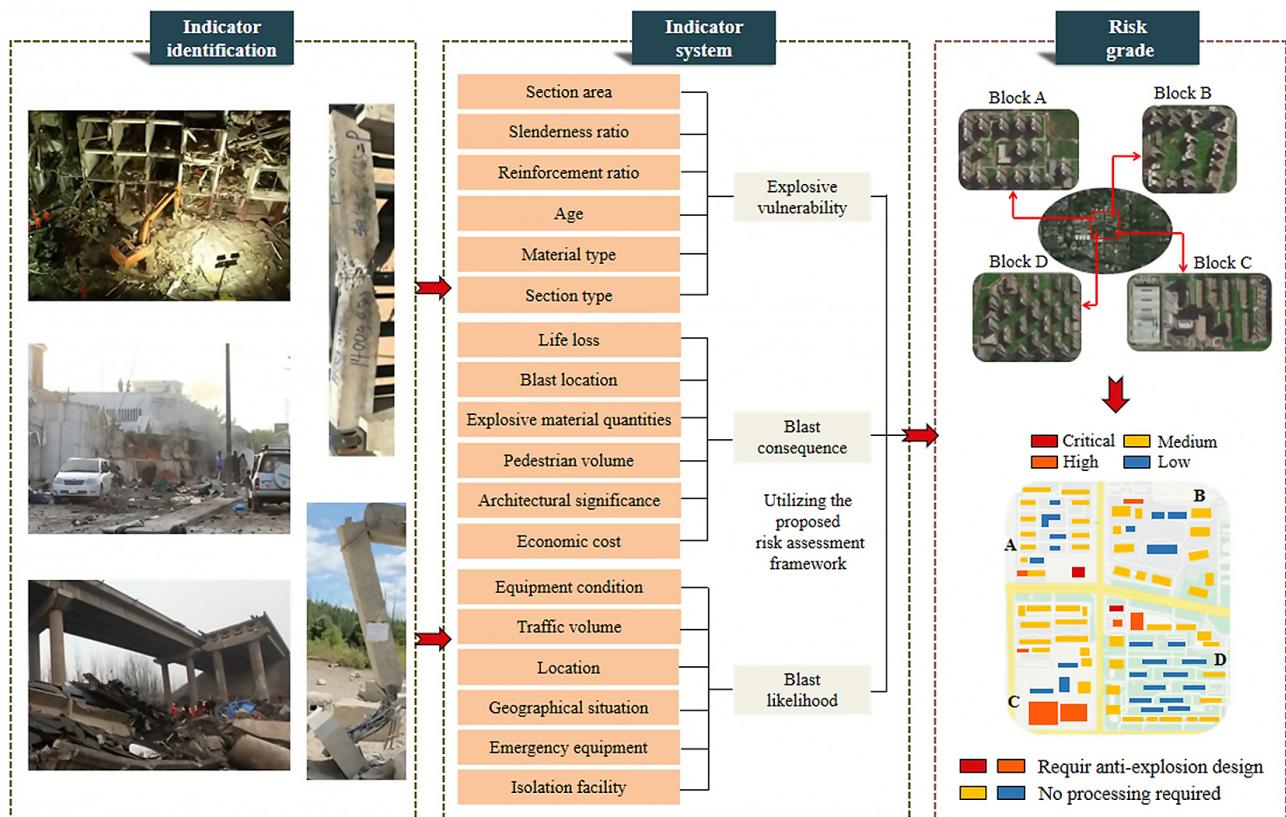


Figure 1. Indicator system of blast risk assessment for structural columns

ural failure, while those with a low slenderness ratio may experience shear failure (Yu et al., 2019). Given the effect of the shear span ratio on the failure mode (Miao et al., 2022), this attribute can be classified under five ranges: < 3, between 3 and 6, between 6 and 9, between 9 and 12, and > 12.

- Reinforcement ratio (C_3)

The longitudinal reinforcement ratio and the volumetric ratio of transverse reinforcement affect the column's blast performance. As the longitudinal reinforcement directly influences the flexural behavior and residual axial capacity of columns, the longitudinal reinforcement ratio is used to evaluate explosive vulnerability. The recommended column longitudinal reinforcement ratio range is 0.6–4% (Sun et al., 2021; Miao et al., 2022). Therefore, this attribute can be < 1.28%, between 1.28 % and 1.96 %, 1.96 % and 2.64 %, 2.64 % and 3.32 %, and > 3.32%.

- Age (C_4)

Both the steel reinforcement and concrete progressively deteriorate over the lifespan of a structure. Consequently, the blast performance diminishes with the aging of the columns. According to current research, the potential age of columns can be 0–15 years, 15–30 years, 30–50 years, or > 50 years (Sun et al., 2021; Andrić & Lu, 2016).

- Material type (C_5)

The blast performance of columns is contingent on the construction materials. Steel materials exhibit robust mechanical properties and energy absorption performance (Al-Thairy, 2018). Generally, steel-concrete composite columns display superior blast performance compared to RC columns (Zhu et al., 2010). Wood components are combustible, so timber columns possess the least explosion resistance (Sun et al., 2021). The explosive vulnerability of RC and masonry columns is regarded as medium and high.

- Section type (C_6)

In practical engineering, the section types of columns predominantly encompass hollow, lattice, solid, and composite sections. Due to their expansive face-on blast surface and thin walls, hollow sections are the most susceptible to damage. The anti-explosion performance of solid columns is superior to that of lattice columns. Composite sections optimally utilize the mechanical properties of each layer, and the inner layer can continue to endure the axial load even after the surface layer is damaged (Sun et al., 2022). Hence, columns with a composite section are considered the least vulnerable under blast loading.

(2) Blast consequence

The ramifications of a blast encompass the detrimental effects resulting from damage to a column. This risk variable is epitomized by the consequences a structure faces when exposed to blast incidents.

- Pedestrian volume (C_7)

The repercussions of an explosion escalate with the pedestrian volume associated with the engineered structure. The quantity of individuals over a specific timeframe

typically denotes pedestrian volume. In accordance with FEMA 426, pedestrian volume can be characterized as fewer than 250 people per day, between 250 and 500 people per day, between 500 and 1000 people per day, between 1000 and 5000 people per day, or over 5000 people per day (Hadjioannou et al., 2018).

- Economic cost (C_8)

The consequences of blast accidents can be gauged by economic losses (Kodur & Naser, 2013). Economic losses are subdivided into direct and indirect costs. Direct economic losses encapsulate maintenance and repair costs, along with damages to goods, while indirect costs entail losses resulting from service disruption, environmental pollution due to explosions, time costs, and others. The economic cost range can be less than 1 million dollars, 1–2 million dollars, 2–3 million dollars, and more than 3 million dollars (Mackie et al., 2009).

- Architectural significance (C_9)

Architectural significance refers to the political and historical importance of engineering structures. The blast repercussions increase with the architectural significance. Structures with pronounced historical and political importance possess high architectural significance. High significance is attributed to national emphasis projects, combat readiness structures, and consular buildings. Medium significance is mainly assigned to landmark engineering structures (Kodur & Naser, 2013), while structures that fulfill certain daily functions (such as medical, transportation, office, or cultural) possess low significance. Common structures are deemed to have very low significance.

- Explosive material quantities (C_{10})

The repercussions of a blast incident are directly proportional to the quantities of explosive materials. The prerequisites for storage methods and reserves of hazardous materials vary across existing specifications (Hadjioannou et al., 2018), making it challenging to evaluate all hazardous materials using a unified index. Consequently, linguistic levels are employed to denote material quantities. The quantity of explosive materials can be none, small, medium, or large.

- Blast location (C_{11})

The extent of damage caused by an explosion fluctuates with the proximity to the blast incident (Sun et al., 2021). Serious consequences arise from blast accidents occurring near columns. Moreover, unfavorable loading positions of components (such as the mid-span of beams and beam-column nodes) hold relative importance, as blasts at critical positions within the structure can engender extensive repercussions. Blasts at common positions within the structure lead to medium consequences. With increasing stand-off distance, the blast overpressure drops swiftly, resulting in minor consequences from blasts occurring not adjacent to the column.

- Life loss (C_{12})

Life loss directly mirrors the consequences of blast incidents. Casualties primarily arise from blast overpressure

and structural collapse. According to Jonkman et al. (2003), the number of lives lost can be 0, 1–3, 3–10, 10–30, or more than 30.

(3) Blast likelihood

This risk parameter is represented by the likelihood of structures facing blast incidents. The explosion accidents considered in this chapter primarily include terrorist attacks and accidental explosions of combustible and explosive materials during production, transportation, storage, and usage.

■ Equipment condition (C_{13})

The process of managing hazardous goods can potentially lead to an accidental explosion due to equipment deterioration (Cao & Lam, 2019). This attribute primarily assesses the equipment used for producing, processing, storing, and utilizing materials. For civil buildings, the equipment primarily includes natural gas pipelines, power lines, and gas tanks. Different equipment specifications exhibit considerable variations. This attribute is evaluated using linguistic levels, and the equipment condition can range from very poor, poor, average, good, to very good.

■ Traffic volume (C_{14})

The likelihood of accidental explosions while transporting hazardous materials escalates with traffic volume. Herein, traffic volume is considered a factor related to explosion possibility. This attribute can be characterized by the daily traffic (ADT) and is divided into five sub-attributes: fewer than 1000 vehicles/day, between 1,000 and 5,000 vehicles/day, between 5,000 and 15,000 vehicles/day, between 15,000 and 50,000 vehicles/day, and more than 50,000 vehicles/day (Kodur & Naser, 2013; Yang et al., 2014).

■ Location (C_{15})

The probability of columns being subject to explosion accidents correlates with the location of the structures. Generally, the chance of explosion accidents surges with the city's size. Based on existing research (Kodur & Naser, 2013), the structure's location can be classified as a metropolis, small-medium city, suburban, or rural area.

■ Geographical situation (C_{16})

Geographical situation accounts for the geopolitics and history of blast incidents (Ding et al., 2013). It is assumed that the threat perception of the region which often suffers from blast incidents is very high, such as the Russia-Ukraine military dispute. The columns within the conflict area are under high blast threat. For instance, a country experiences the internal strife or political instability. In addition, a region with a poor public security and a history of terrorist attacks is considered to be under medium threat perception. For situations where the regional security is good and a few of blast incidents are recorded, the possibility of the columns being subjected to an explosion is low. Further, if strict regulations are established for the storage and transportation of dangerous materials and only professional personnel are

allowed to operate, the columns within the area are with very low threat perception.

■ Emergency equipment (C_{17})

Emergency facilities (e.g., fire extinguishers, ventilation devices, and brake valves) can considerably reduce the likelihood of a blast when hazardous situations such as smoke, ignition sources, and excessive dust transpire. The installation requirements for various emergency facilities differ significantly and cannot be classified using a unified index. Thus, this attribute is described using five linguistic levels (Sun et al., 2021).

■ Isolation facility (C_{18})

Isolation facilities mitigate the likelihood of a blast by distancing columns from explosion sources (Pan et al., 2023). The primary implementation methods encompass: 1) setting up warning signs to restrict vehicles transporting hazardous materials from passing through the engineering structures; 2) using protective facilities (e.g., explosion-proof doors and walls) to segregate explosive materials from the columns. The sub-attributes of this attribute can be categorized as seldom, low, medium, and high.

3.2. Phase 2:

Multi-indicator risk assessment framework

The multi-attribute framework for evaluating the risk levels of columns exposed to blast disasters is illustrated in Figure 2. This framework combines a fuzzy transformation system and a FAHP-based approach. The fuzzy transformation system links the number of sub-attributes to linguistic terms. Based on the membership functions of linguistic term (LTMFs) and the established hierarchical structure, the basic information regarding the columns is converted into fuzzy evaluations. The weights of risk parameters and attributes are derived from the FAHP-based approach. Following this, the defuzzified value is computed through the aggregation and defuzzification of the foundational fuzzy evaluations. The FAHP-based approach encompasses Steps 4–9 of the framework. A detailed process of risk assessment is presented in the paragraph below.

Step 1. Establish the indicator system of risk assessment

As outlined in Section 3.1, the target layer denotes the risk grade, with the subsequent layer indicating the risk parameters, which are determined based on the expression of risk factors (RFs). The lower layers comprise attributes determined by logical inclusion relationships. The sub-attributes of attributes are utilized to evaluate the risk levels of essential indicators. It is necessary for the sub-attributes to cover all columns.

Step 2. Determine the fundamental fuzzy evaluations

The number of sub-attributes determines the type of linguistic term. Thereafter, each attribute is evaluated by the corresponding linguistic term. All types of defined linguistic terms are denoted by $P = \{p_1, p_2, \dots, p_m\}$. The trapezoidal MFs herein are used to describe the linguistic terms. The LTMFs are determined based on the intersection be-

tween different fuzzy scopes of a certain risk grade (Li et al., 2019; Sun et al., 2021). In the non-intersection case, the ordinal scale method is utilized to obtain the points that have a membership degree of 1. The obtained MFs of linguistic terms are denoted as $Q_j = (x, \mu_{Q_j}(x)), x \in R$.

The fuzzy evaluations of attributes are derived, based on the LTMFs and the established hierarchical structure, by comparing column information with corresponding sub-attributes. The fuzzy evaluations of the n th attribute are denoted as $G_n = (G_{n1}, G_{n2}, G_{n3}, G_{n4})$.

Step 3. Calculate the priority weight

Linguistic terms typically employed in pairwise comparisons include moderate, fairly strong, very strong, and absolute (Li et al., 2009; Chan & Kumar, 2007). The precision of the MF shape is usually disregarded due to the inherent ambiguity of the problem (Mottaghi-Kashtiban et al., 2008). Therefore, triangular fuzzy numbers and a linear-shaped membership function suffice to calculate element weights (Andrić & Lu, 2016). The MF can be determined through experimental data, interpretation of linguistic terms, and the nature of the problem (Ahmed & Kilic, 2019). The fuzzy number of a linguistic term can be denoted as $M_{ts} = (m_{ts}^-, m'_{ts}, m_{ts}^+)$.

Subject matter experts convey their judgments on the priority of attributes in pairs (Ahmed & Kilic, 2019). A pairwise comparison matrix among attributes that belong to the same risk parameter is expressed in Eqn (1), where the consistency ratio (CR) of the fuzzy judgment matrix should be smaller than 0.1 (Li et al., 2009; Lyu et al., 2019):

$$X = \begin{pmatrix} M_{11} \cdots M_{1s} \cdots M_{1h} \\ \cdots \\ M_{t1} \cdots M_{ts} \cdots M_{th} \\ \cdots \\ M_{v1} \cdots M_{vs} \cdots M_{vh} \end{pmatrix} \quad (1)$$

Multiple methods for calculating the weight vector of a fuzzy evaluation matrix have been proposed, primarily encompassing the normalized geometric mean approach (Andrić & Lu, 2016; Yang et al., 2014), the extent analysis method (Wang & Elhag, 2006; Chan & Kumar, 2007), and fuzzy classical methods (Nieto-Morote & Ruz-Vila, 2011). The extent analysis method is used here for its straightforward calculation process and ability to compute weight vectors without converting fuzzy numbers into crisp values (Wang & Elhag, 2006; Chan & Kumar, 2007; Shaw et al., 2012). The value of the fuzzy synthetic extent (FSE) of the t th attribute can be calculated as follows (Shaw et al., 2012):

$$S_t = \sum_{s=1}^h M_{ts} \otimes \left[\sum_{s=1}^h \sum_{t=1}^v M_{ts} \right]^{-1};$$

$$\sum_{s=1}^h M_{ts} = \left(\sum_{s=1}^h m_{ts}^-, \sum_{s=1}^h m'_{ts}, \sum_{s=1}^h m_{ts}^+ \right) \quad (2)$$

The weight of the i th attribute is expressed as $w'_i = \min V(S_i \geq S_t)$, where $t = 1, 2, \dots, h$ and $t \neq i$; $V(S_i \geq S_t)$ is the degree of possibility for $S_i(s_i^-, s'_i, s_i^+)$ to be greater than $S_t(s_t^-, s'_t, s_t^+)$, which can be obtained by Eqn (3) (Lee et al., 2009). Both the values of $V(S_i \geq S_t)$ and $V(S_t \geq S_i)$ need to be calculated. The weight vectors are obtained by calculating the degree of possibility for each convex fuzzy number to be greater than others $W' = (w'_1, w'_2, \dots, w'_v)^T$ (Shaw et al., 2012). After normalization, the priority weights of the attributes can be denoted as $W = (w_1, w_2, \dots, w_v)^T$.

$$V(S_i \geq S_t) = \begin{cases} 1, & s_i^- \geq s_t^-, s'_i \geq s'_t, s_i^+ \geq s_t^+; \\ 0, & s_t^- \geq s_i^+ \end{cases};$$

$$V(S_t \geq S_i) = \frac{s_i^- - s_t^+}{(s'_t - s_t^+) - (s'_i - s_i^-)} \quad (3)$$

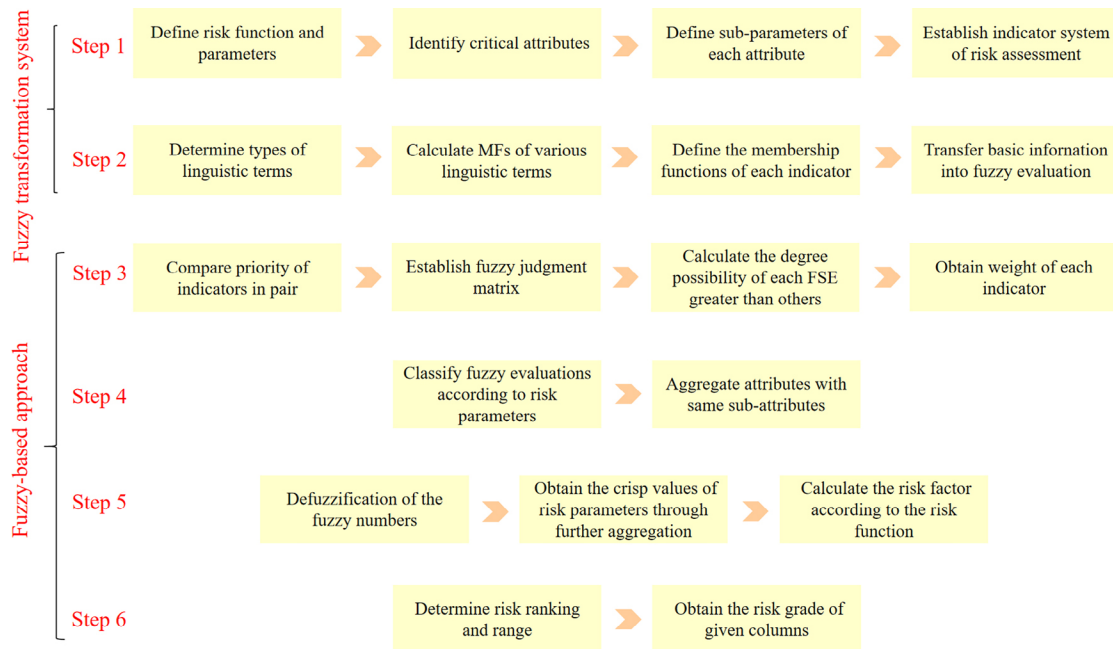


Figure 2. The flowchart for evaluating the risk grade of the columns subjected to blast incidents

Step 4. Aggregate the fuzzy evaluations

After being classified based on the risk parameter, the fuzzy evaluations can be denoted as $G_{jio} = (G_{jio1}, G_{jio2}, G_{jio3}, G_{jio4})$, where j and o stand for the number of sub-attributes and G_{ij} . The fundamental indicators are aggregated as follows (Zeng et al., 2007):

$$G_{ij}^* = (G_{ij1} \otimes w_{ij1} \oplus G_{ij2} \otimes w_{ij2} \oplus \dots \oplus G_{ijm} \otimes w_{ijm}) / (w_{ij1} + \dots + w_{ijm}), \tag{4}$$

where w_{iju} denotes the weight of G_{iju} ; \oplus represents fuzzy addition operator.

Step 5. Calculate the risk factor

The aggregated fuzzy evaluations are first transformed into defuzzified values using the center-of-centroid method (Sun et al., 2021; Shaw et al., 2012). The defuzzified value of G_{ij}^* is represented as CD_{ij} . Thereafter, the defuzzified value of i th parameter is aggregated as follows:

$$AD_i = CD_{i1} * w_{i1} + CD_{i2} * w_{i2} + \dots + CD_{im} * w_{im}, \tag{5}$$

where m is the number of linguistic types.

After obtaining the defuzzified values of the second layer indicators, the RF of a given column can be obtained as follows:

$$RI = f(AD_1, AD_2, \dots, AD_i). \tag{6}$$

Step 6. Determine the risk range and grade

In accordance with existing research and specification requirements, the risk of columns exposed to blast loading is classified into m grades. The boundary values of each grade can be identified by the MFs of linguistic levels, which contain $(m + 1)$ sub-attributes. The risk range is obtained by substituting the boundary values into Eqn (6). Ultimately, the risk level of the columns is determined by comparing the risk range to the RF.

4. Results

This section illustrates the step-by-step application of the proposed framework to five generically designed columns from various engineering structures. Detailed information about these columns and their corresponding engineering structures is provided in Appendix. The primary process of risk assessment of Case 1 is elucidated for conciseness as follows:

Table 2. Fuzzy pairwise comparisons of attributes C_1 – C_6 given by E_1

	C_1	C_2	C_3	C_4	C_5	C_6
C_1	(1, 1, 1)	(2/3, 1, 3/2)	(3/2, 2, 5/2)	(3/2, 2, 5/2)	(2/3, 1, 3/2)	(2/3, 1, 3/2)
C_2	(2/3, 1, 3/2)	(1, 1, 1)	(2/3, 1, 3/2)	(2/3, 1, 3/2)	(2/5, 1/2, 2/3)	(2/3, 1, 3/2)
C_3	(2/5, 1/2, 2/3)	(2/3, 1, 3/2)	(1, 1, 1)	(1, 1, 1)	(2/5, 1/2, 2/3)	(2/3, 1, 3/2)
C_4	(2/5, 1/2, 2/3)	(2/3, 1, 3/2)	(1, 1, 1)	(1, 1, 1)	(2/5, 1/2, 2/3)	(2/3, 1, 3/2)
C_5	(2/3, 1, 3/2)	(3/2, 2, 5/2)	(3/2, 2, 5/2)	(3/2, 2, 5/2)	(1, 1, 1)	(2/3, 1, 3/2)
C_6	(2/3, 1, 3/2)	(2/3, 1, 3/2)	(2/3, 1, 3/2)	(2/3, 1, 3/2)	(2/3, 1, 3/2)	(1, 1, 1)

Note: Consistency check: consistency ratio = 0.042 < 0.1.

Step 1. The determined risk parameters, fundamental indicators, sub-attributes and the indicator system established for blast risk assessment is documented in Section 3.1.

Step 2. This study adopts four levels to assess the risk grade based on prior research (Andrić & Lu, 2016; Zeng et al., 2007): critical, high, medium, and low. Given the number of sub-attributes, the MFs of four and five linguistic terms necessitate computation. For ease of application, the scope of fuzzy evaluation was fixed between 0 and 100. Membership functions for the requisite linguistic terms are obtained using score ranges corresponding to different linguistic levels (Sun et al., 2021; Kodur & Naser, 2013; Tak et al., 2019). Subsequently, fundamental fuzzy evaluations are automatically generated via the transformation system. The fuzzy evaluations (FEVs) for each attribute of Case 1 are listed in Table A.1.

Step 3. The characteristic membership function of the linguistic term, used for the relative importance judgment, was adopted from Kahraman et al. (2004) and Chan and Kumar (2007). The fuzzy numbers employed for pairwise comparisons are listed in Table 1. In this study, five professors in the field of blast risk assessment provided their judgment on pairwise importance comparison. Assuming uniform weighting across experts, the final weight of each attribute is the arithmetic mean. When the weights of experts are different, the FAHP method mentioned above can be employed to determine the weights of individual expert judgments. The fuzzy pairwise comparison matrix of C_1 – C_6 , provided by expert one (E_1), serves as an example to illustrate the weight calculation process (see Table 2). The established pairwise comparison

Table 1. Triangular fuzzy numbers used in pairwise comparisons

Description	Fuzzy number
Equal	(1, 1, 1)
Moderate	(2/3, 1, 3/2)
Fairy strong	(2/3, 2, 5/2)
Very strong	(5/2, 3, 7/2)
Absolute	(7/2, 4, 9/2)

matrix of attributes C_1 – C_6 is documented in Table A.2. The FSE values of attributes C_1 to C_6 were computed according to Eqn (2):

$$S_1 = (0.118, 0.208, 0.356), S_2 = (0.080, 0.143, 0.260), S_3 = (0.081, 0.130, 0.215), S_4 = (0.081, 0.130, 0.215), S_5 = (0.134, 0.234, 0.390), S_6 = (0.085, 0.156, 0.288).$$

The minimum degree of possibility for S_1 to S_6 to be greater than other convex fuzzy numbers are 0.895, 0.580, 0.436, 0.833, 1, and 0.664, respectively. The weight vectors of the example attributes after normalization are $W = (0.223, 0.145, 0.109, 0.109, 0.249, 0.165)^T$. The final weights of attributes C_1 – C_6 are listed in Table A.2, assuming that the importance of each expert is identical. All the pairwise comparison matrices satisfy the consistency requirements.

Step 4. The fuzzy evaluations of the attributes were grouped under three categories based on risk parameters. The attributes with five sub-attributes were aggregated by Eqn (4), taking the parameter B_1 as an example:

$$G_{15}^* = \frac{(25,50,50,75) \otimes 0.271 \oplus (25,50,50,75) \otimes 0.120 \oplus (0,25,25,50) \otimes 0.088 \oplus (25,50,50,75) \otimes 0.250}{0.271 + 0.120 + 0.088 + 0.250} = (22.0, 47.0, 47.0, 72.0).$$

Step 5. The defuzzified value of risk parameter B_7 was aggregated in accordance with Eqn (5). The aggregated fuzzy evaluations of additional risk param-

eters are presented in Table 3. Ultimately, the RF of Case 1 was computed via Eqn (6):

$$AD_1 = 59.6 * 0.271 + 47.2 * 0.729 = 50.6; \\ RI = AD_1 * AD_2 * AD_3 = 208465.7.$$

Step 6. The MFs serve to determine the boundary of the risk grade. The defuzzified values of different linguistic terms were calculated based on the center-of-centroid method. Upon comparison, the boundary values of explosion vulnerability stand at 13.9, 27.1, 50, 72.9, and 86.1. The risk scopes of the risk grades were ascertained employing Eqn (6) and listed in Table 4. Given that the RF falls within the scope of 125000–387686.3, the risk grade of this column exposed to blast incidents was categorized as medium. The calculation results in the risk assessment process of all cases are listed in Table 3. The blast risk grades for Cases 2 to 5 are depicted in Figure 3 by repeating Steps 1–6. The section area of Cases 5 is large and the slenderness ratio is small. The column is located in a rural area of Africa with low traffic volume, so the risk grade of Case 5 is low. Case 3 has a large slenderness ratio and belongs to a landmark building in Kharkiv, Ukraine. The traffic volume is high, and the blast location is generally a key position. Thus, the risk grade of Case 3 is high.

Table 3. The calculation results of each step in risk assessment

Aggregation value	G_{14}^*	G_{15}^*	G_{24}^*	G_{25}^*	G_{34}^*	G_{35}^*
Case 1	(32.5, 52.5, 61.7, 86.2)	(22.0, 47.0, 47.0, 72.0)	(52.5, 75.0, 82.3, 97.1)	(37.9, 62.9, 62.9, 87.9)	(40.0, 60.0, 69.0, 95.0)	(36.3, 61.3, 61.3, 86.3)
Case 2	(61.7, 86.2, 92.2, 98.7)	(20.9, 45.9, 45.9, 70.9)	(26.8, 48.5, 57.1, 71.4)	(24.2, 49.2, 49.2, 74.2)	(20.8, 40.8, 50.4, 72.6)	(27.8, 52.8, 52.8, 77.8)
Case 3	(61.7, 86.2, 92.2, 98.7)	(14.6, 26.2, 26.2, 51.2)	(10.0, 30.0, 40.0, 60.0)	(5.7, 30.7, 30.7, 55.7)	(0.0, 0.0, 10.0, 30.0)	(4.6, 23.0, 23.0, 48.0)
Case 4	(32.5, 52.5, 61.7, 86.2)	(12.7, 34.7, 34.7, 59.7)	(60.8, 85.1, 91.2, 98.6)	(38.7, 63.7, 63.7, 88.7)	(47.8, 71.7, 78.5, 85.6)	(33.3, 53.6, 53.6, 78.6)
Case 5	(47.3, 68.8, 76.8, 96.3)	(53.0, 78.0, 78.0, 100)	(60.8, 85.1, 91.2, 98.6)	(50.0, 75.0, 75.0, 100.0)	(47.8, 71.7, 78.5, 100.0)	(58.3, 83.3, 83.3, 95.4)
Defuzzified value	CD_{14}	CD_{15}	CD_{24}	CD_{25}	CD_{34}	CD_{35}
Case 1	59.6	47.2	72.3	61.8	64.3	60.4
Case 2	79.8	46.2	51.2	50.6	46.0	51.5
Case 3	79.8	30.3	36.8	32.3	18.9	26.9
Case 4	59.6	42.9	79.4	62.5	68.0	54.2
Case 5	75.0	73.9	79.4	72.9	68.0	75.5
Risk parameter	AD_1		AD_2		AD_3	
Case 1	50.6		67.1		61.5	
Case 2	55.3		50.6		50.0	
Case 3	43.7		34.5		24.7	
Case 4	42.9		71.0		58.0	
Case 5	74.2		76.2		73.4	

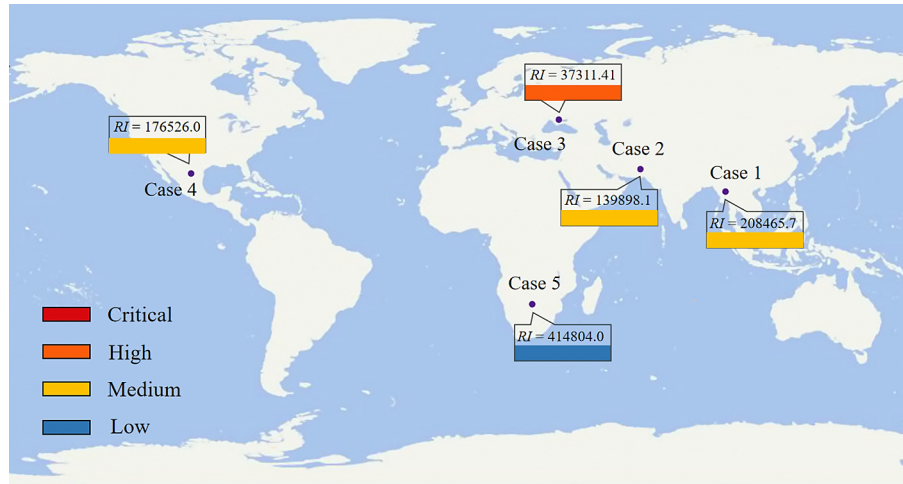


Figure 3. Risk grade of the case columns

5. Discussion

The problem of multi-attribute risk assessment for columns subjected to blast loading can be addressed via a fuzzy-based framework. These fuzzy evaluations represent linguistic variables correlated with the sub-attributes. The suggested risk assessment framework adapts to different column types. After obtaining the risk grade, the importance coefficient can be introduced to enhance the state of design for structural columns. According to the research results of Kodur and Naser (2013), the important factors of associated risk grades are listed in Table 4. For columns requiring blast-resistant design in practical engineering, the blast risk level is first calculated using the proposed method. For columns categorized as high-risk grade, the blast loading needs to be multiplied by a coefficient of 1.2.

Figure 4 compares the attribute weights calculated using FAHP and entropy methods. Although the consistency ratio of the pairwise comparison matrix satisfies the consistency check, the FAHP method requires subjective judgment and is limited by expert knowledge. The precision of the weights used for aggregation improves with the augmentation of comparison matrices. It is assumed that the indicators with more sub-attributes have higher weight (Sun et al., 2021; Kodur & Naser, 2013). The basic information of enough case columns is converted into fuzzy numbers, the results obtained using the entropy method show that the weights of the attributes under each risk parameter and with the same number of sub-attributes are almost the same. For the ob-

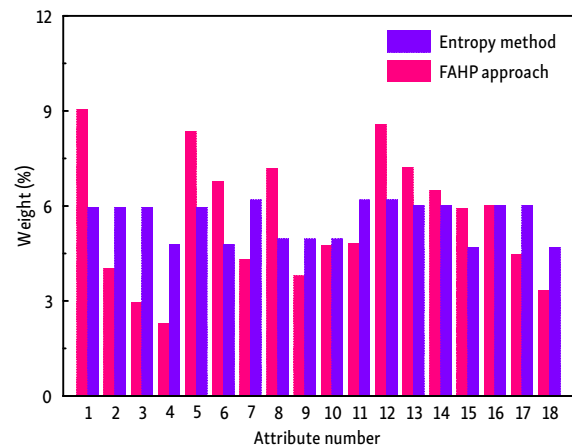


Figure 4. The weights of critical attributes obtained by different methods

jective methods, it is necessary to find a unified index to quantify the impact of each attribute and determine the weight based on the impact degree. The FAHP method seems more reasonable because the dispersion degree of statistical data can not represent the entropy weight of the corresponding attribute. With the expansion of the expert database, the calculation results of attribute weights will progressively align with the actual scenarios.

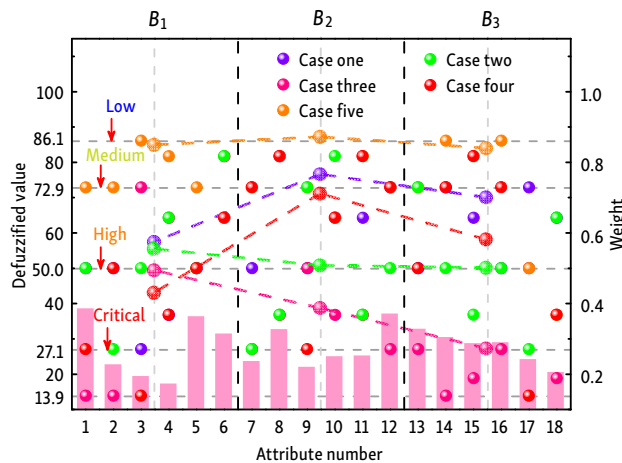
The calibration of the method is accomplished by comparing the computed risk grades of identical cases under disparate frameworks. Based on the essential case information cited in Zeng et al. (2007), the risk grade derived from the proposed method is high. Evaluation results computed indicate a high-risk level probability of 51.3%.

Table 4. Importance factors for anti-explosion design of structural columns

Risk grade	Crisp value of FEVs	Risk range	Importance coefficient
Critical	13.9–27.1	2679.2–19865.8	1.5
High	27.1–50.0	19865.8–125000	1.2
Medium	50.0–72.9	125000–387686.3	1.0
Low	72.9–86.1	387686.3–638524.6	0.8

Table 5. Comparison of risk levels assessed through different approaches

Case in Zeng et al. (2007)		Case in Sun et al. (2021)		Case in Andrić and Lu (2016)	
Method	Risk grade	Method	Risk grade	Method	Risk grade
Zeng et al. (2007)	High	Sun et al. (2021)	Low	Andrić and Lu (2016)	Medium
The proposed method	High	The proposed method	Low	The proposed method	Medium

**Figure 5.** Risk level of each attribute and risk parameter

Risk grades for the cases mentioned in Andrić and Lu (2016) and Sun et al. (2021) are medium and low, respectively. The weights of the influence factors and hazards are integrated into the proposed method, with the risk assessment outcomes detailed in Table 5. The risk grade results obtained through different methods display a reasonable consistency.

As illustrated in Figure 3, the majority of cases fall within the medium-risk level. This is primarily due to the medium grade's wider risk range compared to that of the high and critical grades. Furthermore, the likelihood of extreme situations appearing in the column basic information is comparatively low. The risk grade for columns in metropolitan areas exceeds those in rural locales, predominantly due to highly weighted attributes such as economic and human losses, equipment conditions, and traffic volume, coupled with unfavorable fuzzy evaluations. Figure 5 displays the MF of the attributes relative to the risk level. This framework can prioritize the significance of the attributes. The precise values of the risk parameters aid in comprehending the overall risk levels of the column. In general, modifying the sub-attributes of critical indicators under low crisp value risk parameters for columns identified as high-risk can effectively control the blast risk. For instance, improving the equipment condition and increasing the section area can reduce the risk level in Case 3. The framework offers viable strategies for emergency management.

The fundamental information regarding columns changes over time. The proposed framework can perform dynamic risk level identification and controlling for a column exposed to blast incidents by amalgamating the fundamental fuzzy evaluations. For safety considerations, the

risk grade of all columns within a structure can be represented by the load-bearing column exhibiting the highest vulnerability. The framework can be applied for dynamic monitoring of blast risk on the columns. Furthermore, identifying risk grade provides a foundation for further anti-explosion capacity checks and the selection of strengthening strategies. In the case of high risk columns, the column's risk grades declined following a period of traffic restrictions, personnel evacuation, and equipment updates. Moreover, installing alarm systems and jacketing with protective structures can effectively control the risk grade. These findings hold a certain significance for the anti-explosion design of columns.

6. Conclusions

This study proposes a fuzzy-based risk assessment framework for structural columns threatened by blast incidents. This method integrates a fuzzy transformation system, FAHP weight approach, and a multi-attribute risk assessment method within a comprehensive methodological framework. The primary conclusions are as follows:

1. The factors influencing blast outcomes, column blast performance, and blast probability were summarized and analyzed, leading to the establishment of an indicator system for blast risk assessment.
2. Through a series of case studies, it was proved that this framework can accommodate various linguistic types, calculate the risk range quantitatively, and acquire the desired risk grades for the columns in a logical manner.
3. The framework facilitates the dynamic monitoring and controlling of the blast risk level. It provides a convenient tool for engineers to develop effective and adaptable risk prevention strategies.
4. The framework can be extrapolated to assess the risks of various hazards in other fields. However, the weight determination requires subjective judgment and the basic information of the column needs to be collected in the risk assessment process. In our future work, the machine learning approach will be utilized to process enough explosion accidents and existing literature for obtaining the pairwise comparison matrix. The qualitative and quantitative risk assessment methods will be combined in our framework. Moreover, we will explore the statistical indicators covering the entire city to achieve a national blast risk distribution.

Acknowledgements

The study is supported by the National Natural Science Foundation of China (No. 52078169).

Competing interests

The authors declare that they have no known competing financial interests or personal relationships that could have appeared to influence the work reported in this paper.

References

- Abdollahzadeh, G., & Faghihmaleki, H. (2017). Probabilistic two-hazard risk assessment of near-fault and far-fault earthquakes in a structure subjected to earthquake-induced gas explosion. *Journal of Building Engineering*, *13*, 298–304. <https://doi.org/10.1016/j.jobe.2017.09.002>
- Ahmed, F., & Kilic, K. (2019). Fuzzy analytic hierarchy process: A performance analysis of various algorithms. *Fuzzy Sets and Systems*, *362*, 110–128. <https://doi.org/10.1016/j.fss.2018.08.009>
- Al-Thairy, H. (2016). A modified single degree of freedom method for the analysis of building steel columns subjected to explosion induced blast load. *International Journal of Impact Engineering*, *94*, 120–133. <https://doi.org/10.1016/j.ijimpeng.2016.04.007>
- Al-Thairy, H. (2018). Behaviour and failure of steel columns subjected to blast loads: Numerical study and analytical approach. *Advances in Materials Science and Engineering*, *2018*, Article 1591384. <https://doi.org/10.1155/2018/1591384>
- Andrić, J. M., & Lu, D. (2016). Risk assessment of bridges under multiple hazards in operation period. *Safety Science*, *83*, 80–92. <https://doi.org/10.1016/j.ssci.2015.11.001>
- Attary, N., Unnikrishnan, V. U., van de Lindt, J. W., Daniel, T. C., & Barbosa, A. R. (2017). Performance-based tsunami engineering methodology for risk assessment of structures. *Engineering Structures*, *141*, 676–686. <https://doi.org/10.1016/j.engstruct.2017.03.071>
- Cao, X., & Lam, J. S. L. (2019). A fast reaction-based port vulnerability assessment: Case of Tianjin Port explosion. *Transportation Research Part A: Policy and Practice*, *128*, 11–33. <https://doi.org/10.1016/j.tra.2019.05.019>
- Chan, F. T. S., & Kumar, N. (2007). Global supplier development considering risk factors using fuzzy extended AHP-based approach. *Omega*, *35*(4), 417–431. <https://doi.org/10.1016/j.omega.2005.08.004>
- Chen, S. (2001). Fuzzy group decision making for evaluating the rate of aggregative risk in software development. *Fuzzy Sets and Systems*, *118*(1), 75–88. [https://doi.org/10.1016/S0165-0114\(99\)00103-7](https://doi.org/10.1016/S0165-0114(99)00103-7)
- Chen, D. (2021). Risk assessment of government debt based on machine learning algorithm. *Complexity*, *2021*, Article 3686692. <https://doi.org/10.1155/2021/3686692>
- Cho, J., Jang, S., & Song, J. (2023). Onsite measurement and dilution-based infection risk assessment for a new mobile negative pressure isolation room (MNPIR) as a solution to minimize cross-infection. *Sustainable Cities and Society*, *95*, Article 104583. <https://doi.org/10.1016/j.scs.2023.104583>
- Clough, L. G., & Clubley, S. K. (2019). Steel column response to thermal and long duration blast loads inside an air blast tunnel. *Structure and Infrastructure Engineering*, *15*(11), 1510–1528. <https://doi.org/10.1080/15732479.2019.1635627>
- Davidson, V. J., Ryks, J., & Fazil, A. (2006). Fuzzy risk assessment tool for microbial hazards in food systems. *Fuzzy Sets and Systems*, *157*(9), 1201–1210. <https://doi.org/10.1016/j.fss.2005.12.018>
- Ding, Y., Fang, L., Li, Z., & Shi, Y. (2013). Research on categorized explosion protection criterion of anti-terrorism building structures. *Journal of Building Structures*, *34*(4), 57–64.
- Ezcurra, M. D. (2024). Exploring the effects of weighting against homoplasy in genealogies of palaeontological phylogenetic matrices. *Cladistics*, *40*(3), 242–281. <https://doi.org/10.1111/cla.12581>
- Faber, M. H., & Stewart, M. G. (2003). Risk assessment for civil engineering facilities: critical overview and discussion. *Reliability Engineering and System Safety*, *80*, 173–184. [https://doi.org/10.1016/S0951-8320\(03\)00027-9](https://doi.org/10.1016/S0951-8320(03)00027-9)
- Gündel, M., Hoffmeister, B., Feldmann, M., & Hauke, B. (2012). Design of high rise steel buildings against terrorist attacks. *Computer-Aided Civil & Infrastructure Engineering*, *27*(5), 369–383. <https://doi.org/10.1111/j.1467-8667.2011.00749.x>
- Hadjioannou, M., Donahue, S., Williamson, E. B., & Engelhardt, M. D. (2018). Large-scale experimental tests of composite steel floor systems subjected to column loss scenarios. *Journal of Structural Engineering*, *144*(2), Article 04017184. [https://doi.org/10.1061/\(ASCE\)ST.1943-541X.0001929](https://doi.org/10.1061/(ASCE)ST.1943-541X.0001929)
- Hou, X., Cao, S., Rong, Q., & Zheng, W. (2018). A P-I diagram approach for predicting failure modes of RPC one-way slabs subjected to blast loading. *International Journal of Impact Engineering*, *120*, 171–184. <https://doi.org/10.1016/j.ijimpeng.2018.06.006>
- Ji, Y., Huang, G. H., & Sun, W. (2015). Risk assessment of hydropower stations through an integrated fuzzy entropy-weight multiple criteria decision making method: A case study of the Xiangxi River. *Expert Systems with Applications*, *42*, 5380–5389. <http://doi.org/10.1016/j.eswa.2014.12.026>
- Jonkman, S. N., van Gelder, P. H. A. J. M., & Vrijling, J. K. (2003). An overview of quantitative risk measures for loss of life and economic damage. *Journal of Hazardous Materials*, *99*(1), 1–30. [https://doi.org/10.1016/S0304-3894\(02\)00283-2](https://doi.org/10.1016/S0304-3894(02)00283-2)
- Kahraman, C., Cebeci, U., & Ruan, D. (2004). Multi-attribute comparison of catering service companies using fuzzy AHP: The case of Turkey. *International Journal of Production Economics*, *87*(2), 171–184. [https://doi.org/10.1016/S0925-5273\(03\)00099-9](https://doi.org/10.1016/S0925-5273(03)00099-9)
- Karimi, I., & Hüllermeier, E. (2007). Risk assessment system of natural hazards: A new approach based on fuzzy probability. *Fuzzy Sets and Systems*, *158*(9), 987–999. <https://doi.org/10.1016/j.fss.2006.12.013>
- Kodur, V. K. R., & Naser, M. Z. (2013). Importance factor for design of bridges against fire hazard. *Engineering Structures*, *54*, 207–220. <https://doi.org/10.1016/j.engstruct.2013.03.048>
- Kong, H., & Zhang, N. (2024). Risk assessment of water inrush accident during tunnel construction based on FAHP-I-TOPSIS. *Journal of Cleaner Production*, *449*, Article 141744. <https://doi.org/10.1016/j.jclepro.2024.141744>
- Koohathongsumrit, N., & Meethom, W. (2024). Risk analysis in underground tunnel construction with tunnel boring machines using the Best–Worst method and data envelopment analysis. *Heliyon*, *10*(1), Article e23486. <https://doi.org/10.1016/j.heliyon.2023.e23486>
- Lee, A. H. I., Kang, H. Y., Hsu, C. F., & Hung, H. C. (2009). A green supplier selection model for high-tech industry. *Expert Systems with Applications*, *36*(4), 7917–7927. <https://doi.org/10.1016/j.eswa.2008.11.052>
- Li, L., Shi, Z., Yin, W., Zhu, D., Ng, S., Cai, C., & Lei, A. (2009). A fuzzy analytic hierarchy process (FAHP) approach to eco-environmental vulnerability assessment for the Danjiangkou

- reservoir area, China. *Ecological Modelling*, 220(23), 3439–3447. <https://doi.org/10.1016/j.ecolmodel.2009.09.005>
- Li, J., Zhang, J., & Suo, W. (2019). Risk assessment in cross-border transport infrastructure projects: A fuzzy hybrid method considering dual interdependent effects. *Information Sciences*, 488, 140–157. <https://doi.org/10.1016/j.ins.2019.03.028>
- Li, C., Qiao, Z., Hao, M., Zhang, H., & Li, G. (2022). Effect of ignition energy on environmental parameters of gas explosion in semiclosed pipeline. *ACS Omega*, 7(12), 10394–10405. <https://doi.org/10.1021/acsomega.1c07097>
- Lyu, H., Shen, S., Zhou, A., & Zhou, W. (2019). Flood risk assessment of metro systems in a subsiding environment using the interval FAHP-FCA approach. *Sustainable Cities and Society*, 50, Article 101682. <https://doi.org/10.1016/j.scs.2019.101682>
- Mackie, K. R., Wong, J. M., & Stojadinovic, B. (2009). Post-earthquake bridge repair cost and repair time estimation methodology. *Earthquake Engineering & Structural Dynamics*, 39(3), 281–301. <https://doi.org/10.1002/eqe.942>
- Miao, L., Jin, L., Li, D., Du, X., & Zhang, B. (2022). Effect of shear-span ratio and vertical reinforcement ratio on the failure of geometrical-similar RC shear walls. *Engineering Failure Analysis*, 139, Article 106407. <https://doi.org/10.1016/j.engfailanal.2022.106407>
- Mottaghi-Kashtiban, M., Khoei, A., & Hadidi, K. (2008). Optimization of rational-powered membership functions using extended Kalman filter. *Fuzzy Sets and Systems*, 159(23), 3232–3244. <https://doi.org/10.1016/j.fss.2008.06.021>
- Mutlu, M., & Sari, M. (2022). Risk-based classification of underground coal mine basins in Turkey using the analytic hierarchy process (AHP). *Arabian Journal of Geosciences*, 15, Article 752. <https://doi.org/10.1007/s12517-022-10005-9>
- Nieto-Morote, A., & Ruz-Vila, F. (2011). A fuzzy approach to construction project risk assessment. *International Journal of Project Management*, 29(2), 220–231. <https://doi.org/10.1016/j.ijproman.2010.02.002>
- Ouyang, M. (2014). Review on modeling and simulation of interdependent critical infrastructure systems. *Reliability Engineering & System Safety*, 121, 43–60. <https://doi.org/10.1016/j.res.2013.06.040>
- Pan, R., Cui, B., Zhang, X., Wang, Y., & Zheng, L. (2023). Study on pressure wave response and overpressure attenuation law of explosion-proof doors. *Process Safety and Environmental Protection*, 169, 706–717. <https://doi.org/10.1016/j.psep.2022.11.032>
- Pérez-Fernández, R., Alonso, P., Díaz, I., & Montes, S. (2015). Multi-factorial risk assessment: An approach based on fuzzy preference relations. *Fuzzy Sets and Systems*, 278, 67–80. <https://doi.org/10.1016/j.fss.2014.10.012>
- Qi, S., Du, Y., Zhang, P., Li, G., Zhou, Y., & Wang, B. (2017). Effects of concentration, temperature, humidity, and nitrogen inert dilution on the gasoline vapor explosion. *Journal of Hazardous Materials*, 323, 593–601. <https://doi.org/10.1016/j.jhazmat.2016.06.040>
- Qie, Z., & Rong, L. (2017). An integrated relative risk assessment model for urban disaster loss in view of disaster system theory. *Natural Hazards*, 88, 165–190. <https://doi.org/10.1007/s11069-017-2861-z>
- Qin, H., & Stewart, M. G. (2020). Wind and rain losses for metal-roofed contemporary houses subjected to non-cyclonic windstorms. *Structural Safety*, 86, Article 101979. <https://doi.org/10.1016/j.strusafe.2020.101979>
- Ravankhah, M., Schmidt, M., & Will, T. (2021). An indicator-based risk assessment framework for World Heritage sites in seismic zones: The case of “Bam and its Cultural Landscape” in Iran. *International Journal of Disaster Risk Reduction*, 63, Article 102405. <https://doi.org/10.1016/j.ijdrr.2021.102405>
- Shaw, K., Shankar, R., Yadav, S. S., & Thakur, L. S. (2012). Supplier selection using fuzzy AHP and fuzzy multi-objective linear programming for developing low carbon supply chain. *Expert Systems with Applications*, 39, 8182–8192. <https://doi.org/10.1016/j.eswa.2012.01.149>
- Shi, Y., & Stewart, M. G. (2015). Spatial reliability analysis of explosive blast load damage to reinforced concrete columns. *Structural Safety*, 53, 13–25. <https://doi.org/10.1016/j.strusafe.2014.07.003>
- Shi, Y., Li, Z., & Hao, H. (2010). A new method for progressive collapse analysis of RC frames under blast loading. *Engineering Structures*, 32(6), 1691–1703. <https://doi.org/10.1016/j.engstruct.2010.02.017>
- Stawczyk, J. (2003). Experimental evaluation of LPG tank explosion hazards. *Journal of Hazardous Materials*, 96(2–3), 189–200. [https://doi.org/10.1016/S0304-3894\(02\)00198-X](https://doi.org/10.1016/S0304-3894(02)00198-X)
- Stewart, M. G., & Netherton, M. D. (2008). Security risks and probabilistic risk assessment of glazing subject to explosive blast loading. *Reliability Engineering & System Safety*, 93(4), 6278–638. <https://doi.org/10.1016/j.res.2007.03.007>
- Sun, P., Hou, X., Zheng, W., Qin, H., & Shao, G. (2021). Risk assessment for bridge structures against blast hazard via a fuzzy-based framework. *Engineering Structures*, 232, Article 111874. <https://doi.org/10.1016/j.engstruct.2021.111874>
- Sun, P., Hou, X., Zheng, W., & Cao, S. (2022). Strengthening of conventional columns through RPC sandwich tube against blast loading. *Structures*, 45, 1850–1863. <https://doi.org/10.1016/j.istruc.2022.09.115>
- Tak, H. Y., Suh, W., & Lee, Y. J. (2019). System-level seismic risk assessment of bridge transportation networks employing probabilistic seismic hazard analysis. *Mathematical Problems in Engineering*, 2019, Article 6503616. <https://doi.org/10.1155/2019/6503616>
- Takaki, Y., & Gotoh, K. (2020). Approximate weight functions of stress intensity factor for a wide range shapes of surface and an embedded elliptical crack. *Marine Structures*, 70, Article 102696. <https://doi.org/10.1016/j.marstruc.2019.102696>
- Tang, Y., Dai, G., Zhou, Y., Huang, Y., & Zhou, D. (2023). Conflicting evidence fusion using a correlation coefficient-based approach in complex network. *Chaos, Solitons & Fractals*, 176, Article 114087. <https://doi.org/10.1016/j.chaos.2023.114087>
- Tang, Y., Sun, Z., Zhou, D., & Huang, Y. (2024). Failure mode and effects analysis using an improved pignistic probability transformation function and grey relational projection method. *Complex & Intelligent Systems*, 10(2), 2233–2247. <https://doi.org/10.1007/s40747-023-01268-0>
- Tetougueni, C. D., Zampieri, P., & Pellegrino, C. (2020). Structural performance of a steel cable-stayed bridge under blast loading considering different stay patterns. *Engineering Structures*, 219, Article 110739. <https://doi.org/10.1016/j.engstruct.2020.110739>
- Valdano, E., Poletto, C., Giovannini, A., Palma, D., Savini, L., & Colizza, V. (2015). Predicting epidemic risk from past temporal contact data. *Plos Computational Biology*, 11(3), Article e1004152. <https://doi.org/10.1371/journal.pcbi.1004152>
- Wang, Y., & Elhag, T. M. S. (2006). Fuzzy TOPSIS method based on alpha level sets with an application to bridge risk assessment. *Expert Systems with Applications*, 31, 309–319. <https://doi.org/10.1016/j.eswa.2005.09.040>
- Wang, Y., & Elhag, T. M. S. (2007). A fuzzy group decision making approach for bridge risk assessment. *Computers & Industrial Engineering*, 53(1), 137–148. <https://doi.org/10.1016/j.cie.2007.04.009>

- Wang, X., & Zhang, Z. (2022). Residual axial capacity of square recycled aggregate concrete-filled steel tube columns after blast loads. *Journal of Building Engineering*, 47, Article 103865. <https://doi.org/10.1016/j.jobe.2021.103865>
- Wang, Y., Li, Z., Tang, Z., & Zeng, G. (2011). A GIS-based spatial multi-criteria approach for flood risk assessment in the Dongting lake region, Hunan, central China. *Water Resources Management*, 25, 3465–3484. <http://doi.org/10.1007/s11269-011-9866-2>
- Yan, Y., Hou, X., Zheng, W., & Fei, H. (2022). The damage response of RC columns with considering different longitudinal and shear reinforcement under demolition blasting. *Journal of Building Engineering*, 62, Article 105396. <https://doi.org/10.1016/j.jobe.2022.105396>
- Yang, B., Wang, S., & Bao, Y. (2014). New efficient regression method for local AADT estimation via SCAD variable selection. *IEEE Transactions on Intelligent Transportation Systems*, 15(6), 2726–2731. <https://doi.org/10.1109/TITS.2014.2318039>
- Yu, R., Chen, L., Fang, Q., Yan, H., & Chen, G. (2019). Generation of pressure-impulse diagrams for failure modes of RC columns subjected to blast loads. *Engineering Failure Analysis*, 100, 520–535. <https://doi.org/10.1016/j.engfailanal.2019.02.001>
- Zeng, J., An, M., & Smith, N. J. (2007). Application of a fuzzy based decision making methodology to construction project risk assessment. *International Journal of Project Management*, 25(6), 589–600. <https://doi.org/10.1016/j.ijproman.2007.02.006>
- Zhen, Y., Liu, S., Zhong, G., Zhou, Z., Liang, J., Zheng, W., & Fang, Q. (2022). Risk assessment of flash flood to buildings using an indicator-based methodology: a case study of mountainous rural settlements in southwest China. *Frontiers in Environmental Science*, 10, Article 931029. <https://doi.org/10.3389/fenvs.2022.931029>
- Zhou, X., Huang, B., Wang, X., & Xia, Y. (2022). Deep learning-based rapid damage assessment of RC columns under blast loading. *Engineering Structures*, 271, Article 114949. <https://doi.org/10.1016/j.engstruct.2022.114949>
- Zhu, M., Liu, J., Wang, Q., & Feng, X. (2010). Experimental research on square steel tubular columns filled with steel-reinforced self-consolidating high-strength concrete under axial load. *Engineering Structures*, 32(8), 2278–2286. <https://doi.org/10.1016/j.engstruct.2010.04.002>

APPENDIX

Basic information about case study

The basic information of the five case columns and the fuzzy evaluations of Case 1 are listed in Table A.1.

Table A.1. Basic information of the columns in the case study

Attributes	Sub-attributes					
	Case 1	Case 2	Case 3	Case 4	Case 5	FEVs of Case 1
Section area	1.10×1.10 m	$r = 1.20$ m	0.40×0.40 m	$r = 0.8$ m	1.6×1.6 m	(25, 50, 50, 75)
Slenderness ratio	6.8	10.0	13.5	7.5	4.3	(25, 50, 50, 75)
Longitudinal reinforcement ratio	1.52%	2.16%	3.21%	0.82%	4.84%	(0, 25, 25, 50)
Age (years)	30–50	15–30	15–30	30–50	0–15	(10, 30, 40, 60)
Material type	RC	RC	RC	RC	Steel-concrete composite	(25, 50, 50, 75)
Section type	Solid	Composite	Composite	Solid	Solid	(40, 60, 69, 95)
Pedestrian volume (people/day)	500–1000	1000–5000	1000–5000	250–500	250–500	(0, 25, 25, 50)
Economic cost (million dollars)	<1	2–3	2–3	<1	<1	(69, 95, 100, 100)
Architectural significance	Landmark	Office	Landmark	Combat readiness	Amusement	(25, 50, 50, 75)
Explosive material quantities	Small	No	Medium	Small	Small	(40, 60, 69, 95)
Blast location	Common position	Key position	Key position	A certain distance apart	A certain distance apart	(40, 60, 69, 95)
Life loss	1–3	3–10	10–30	1–3	1–3	(50, 75, 75, 100)
Equipment condition	Medium	Good	Bad	Medium	Good	(25, 50, 50, 75)
Traffic volume (vehicles/day)	1,000–5,000	5,000–15,000	50,000	1,000–5,000	< 1000	(50, 75, 75, 100)
Location	Suburban	Small-medium city	Metropolis	Rural area	Rural area	(40, 60, 69, 95)
Geographical situation	Medium	Medium	High	Low	Very low	(25, 50, 50, 75)
Emergency equipment	High	Low	Medium	Very low	Medium	(50, 75, 75, 100)
Isolation facility	Medium	Medium	Seldom	Low	Low	(40, 60, 69, 95)

The fuzzy pairwise comparisons of attributes C_1 – C_6 given by E_2 – E_5 are listed in Table A.2.

Table A.2. Weight of the attributes under risk parameter B_1

	C_1	C_2	C_3	C_4	C_5	C_6	Consistency ratio
E_2	(1, 1, 1)	(2/3, 1, 3/2)	(3/2, 2, 5/2)	(3/2, 2, 5/2)	(3/2, 2, 5/2)	(3/2, 2, 5/2)	0.037
	(2/3, 1, 3/2)	(1, 1, 1)	(1, 1, 1)	(3/2, 2, 5/2)	(2/3, 1, 3/2)	(2/3, 1, 3/2)	
	(2/5, 1/2, 2/3)	(1, 1, 1)	(1, 1, 1)	(3/2, 2, 5/2)	(1, 1, 1)	(2/3, 1, 3/2)	
	(2/5, 1/2, 2/3)	(2/5, 1/2, 2/3)	(2/5, 1/2, 2/3)	(1, 1, 1)	(2/5, 1/2, 2/3)	(2/3, 1, 3/2)	
	(2/5, 1/2, 2/3)	(2/3, 1, 3/2)	(1, 1, 1)	(3/2, 2, 5/2)	(1, 1, 1)	(2/3, 1, 3/2)	
	(2/5, 1/2, 2/3)	(2/3, 1, 3/2)	(2/3, 1, 3/2)	(2/3, 1, 3/2)	(2/3, 1, 3/2)	(1, 1, 1)	
E_3	(1, 1, 1)	(3/2, 2, 5/2)	(3/2, 2, 5/2)	(3/2, 2, 5/2)	(2/3, 1, 3/2)	(1, 1, 1)	0.033
	(2/5, 1/2, 2/3)	(1, 1, 1)	(1, 1, 1)	(2/3, 1, 3/2)	(2/3, 1, 3/2)	(2/3, 1, 3/2)	
	(2/5, 1/2, 2/3)	(1,1,1)	(1, 1, 1)	(2/3, 1, 3/2)	(2/5, 1/2, 2/3)	(2/5, 1/2, 2/3)	
	(2/5, 1/2, 2/3)	(2/3, 1, 3/2)	(2/3, 1,3/2)	(1, 1, 1)	(2/5, 1/2, 2/3)	(2/5, 1/2, 2/3)	
	(2/3, 1, 3/2)	(2/3, 1, 3/2)	(3/2, 2,5/2)	(3/2, 2, 5/2)	(1, 1, 1)	(2/3, 1, 3/2)	
	(1, 1, 1)	(2/3, 1, 3/2)	(3/2, 2, 5/2)	(3/2, 2, 5/2)	(2/3, 1, 3/2)	(1, 1, 1)	
E_4	(1, 1, 1)	(3/2, 2, 5/2)	(3/2, 2, 5/2)	(3/2, 2, 5/2)	(2/3, 1, 3/2)	(1, 1, 1)	0.017
	(2/5, 1/2, 2/3)	(1, 1, 1)	(1, 1, 1)	(2/3, 1, 3/2)	(2/5, 1/2, 2/3)	(2/5, 1/2, 2/3)	
	(2/5, 1/2, 2/3)	(1, 1, 1)	(1, 1, 1)	(2/3, 1, 3/2)	(2/5, 1/2, 2/3)	(2/5, 1/2, 2/3)	
	(2/5, 1/2, 2/3)	(2/3, 1, 3/2)	(2/3, 1, 3/2)	(1, 1, 1)	(2/5, 1/2, 2/3)	(2/5, 1/2, 2/3)	
	(2/3, 1, 3/2)	(3/2, 2, 5/2)	(3/2, 2, 5/2)	(3/2, 2, 5/2)	(1, 1, 1)	(2/3, 1, 3/2)	
	(1, 1, 1)	(3/2, 2, 5/2)	(3/2, 2, 5/2)	(3/2, 2, 5/2)	(2/3, 1, 3/2)	(1, 1, 1)	
E_5	(1, 1, 1)	(3/2, 2, 5/2)	(3/2, 2, 5/2)	(3/2, 2, 5/2)	(1, 1, 1)	(2/3, 1, 3/2)	0.038
	(2/5, 1/2, 2/3)	(1, 1, 1)	(1, 1, 1)	(2/3, 1, 3/2)	(2/5, 1/2, 2/3)	(2/3, 1, 3/2)	
	(2/5, 1/2, 2/3)	(1, 1, 1)	(1, 1, 1)	(2/3, 1, 3/2)	(2/7, 1/3, 2/5)	(2/3, 1, 3/2)	
	(2/5, 1/2, 2/3)	(2/3, 1, 3/2)	(2/3, 1, 3/2)	(1, 1, 1)	(2/5, 1/2, 2/3)	(2/5, 1/2, 2/3)	
	(1, 1, 1)	(3/2, 2, 5/2)	(5/2, 3, 7/2)	(3/2, 2, 5/2)	(1, 1, 1)	(2/3, 1, 3/2)	
	(2/3, 1, 3/2)	(2/3, 1, 3/2)	(2/3, 1, 3/2)	(3/2, 2, 5/2)	(2/3, 1, 3/2)	(1, 1, 1)	
W	0.271	0.120	0.088	0.068	0.250	0.203	